## Supporting Information

# Mineralogy Controlled Dissolution of Uranium from Airborne Dust in Simulated Lung Fluids (SLFs) and Possible Health Implications

*Eshani Hettiarachchi[a], Shaylene Paul[b], Daniel Cadol[c], Bonnie Frey[d], Gayan Rubasinghege[a*]*

*a.* Department of Chemistry, New Mexico Tech, 801 Leroy Place, Socorro, New Mexico 87801.
*b.* Department of Environmental Science, Navajo Technical University, Lowerpoint Road, Crownpoint, New Mexico 87313.
*c.* Department of Earth and Environmental Science, New Mexico Tech, 801 LeRoy Pl, Socorro, New Mexico 87801.
*d.* New Mexico Bureau of Geology, New Mexico Tech, 801 LeRoy Pl, Socorro, New Mexico 87801.
*Corresponding Author: gayan.rubasinghege@nmt.edu

## Locations of the Collected Dust

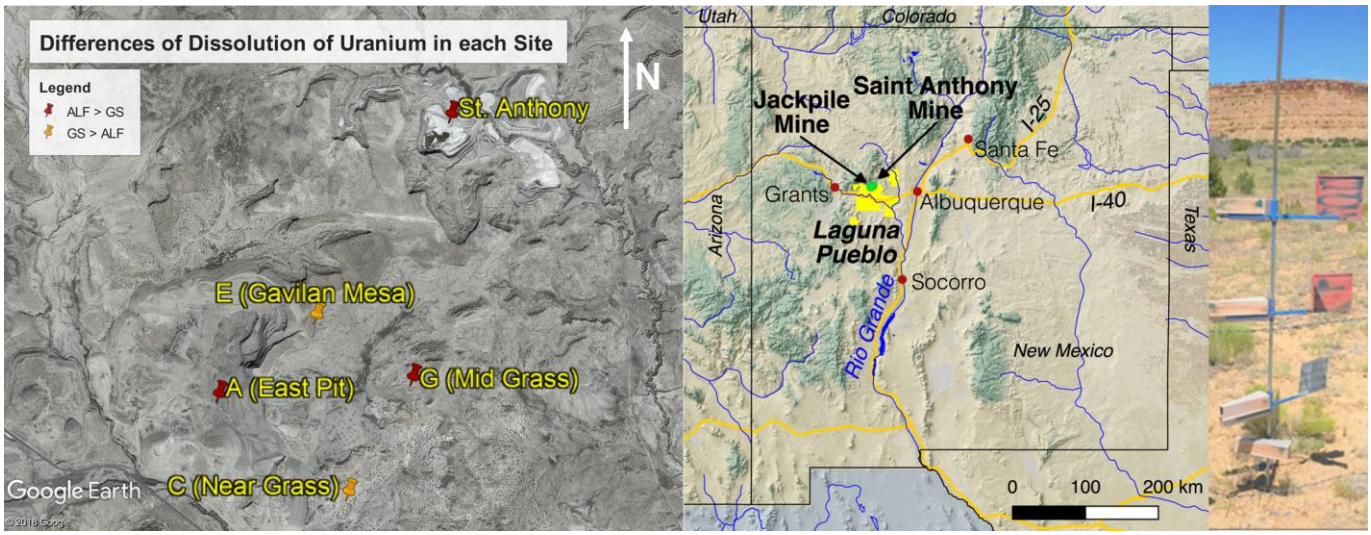


**Figure S1. Dust sample collection locations (left) and area map (center). Picture of four Big Spring Number Eight passive dust collectors at four sampling heights (right). Only the dust from the highest collector, at 1.5 m height, was used in this study. The area map was created using QGIS 2.18 software. Data source: National Map Small Scale Collection, hosted by USGS.**

Dust and sediment samples were collected from different topographies **(Figure S1**) in the vicinity of Jackpile Mine on Laguna Pueblo, New Mexico, and St. Anthony Mine to the north. Overall, the climate is semiarid, with the area receiving most of its annual rainfall during the monsoon season from July to August. The rest of the year is generally dry with occasional snow in the winter. The spring is dominated by winds from the west and northwest. Throughout the year winds from these directions consistently average the highest wind speeds and the highest gust speeds. Though winds come from all directions, the majority of the aeolian transport was expected to be to the southeast of the main pit. During mining operation, sources of the dust included the pit, rock crushers, uncovered waste rock piles, and onsite ore stockpiles.

The Jackpile Mine is located in the Paguate River valley, with mountains to the west and a series of mesas and valleys to the east. Site A, or East Pit, is 40 m thick backfilled with proto-ore and waste rock above the mineralized uranium deposits. This waste rock does not necessarily contain uranium above background.[1] Site E is located at very top of a Gavilan mesa. Site C is located immediate downwind whereas Site G is located the farthest downwind from the Jackpile mine. A continuing major uranium source in the study area is the St. Anthony Mine (0.87% of uranium by mass), an inactive but completely un-remediated mine located ~5 km to the northeast, just north of the Laguna Pueblo boundary.[1]

## List of Chemicals

The following chemicals were used to prepare SLFs according to the composition described in Pelfrene et al.[2] (**Table S1**): sodium chloride (NaCl, Acros, +99.0%), disodium hydrogenphosphate ($Na_2HPO_4$, Sigma-Aldrich, +99.0%), sodium bicarbonate ($NaHCO_3$, Sigma, 99.5%), trisodium citrate dihydrate ($C_6H_5Na_3O_7$, Sigma-Aldrich, +99%), ammonium chloride ($NH_4Cl$, VWR International, 99.5%), glycine ($NH_2CH_2COOH$, Aldrich Chemical Company, +99%), sodium dihydrogen phosphate ($NaH_2PO_4$, Sigma-Aldrich, +99.0%), L-cysteine ($C_3H_7NO_2S$, Aldrich Chemical Company, 99%), sodium hydroxide (NaOH, VWR International, 97%), citric acid monohydrate ($C_6H_8O_7.H_2O$, Fluka Analytical, +99%), calcium chloride dihydrate ($CaCl_2.2H_2O$, Fisher Scientific, +99%), sodium sulfate ($Na_2SO_4$, Sigma-Aldrich, +99%), magnesium chloride hexahydrate ($MgCl_2.6H_2O$, Sigma-Aldrich, +99%), disodium tartrate dihydrate ($C_4H_4Na_2O_6.2H_2O$, Honeywell Riedel – de Haen, 99.5%), sodium L- lactate ($C_3H_5NaO_3$, Sigma, 98%), sodium pyruvate ($C_3H_3NaO_3$, Sigma-Aldrich, +99%). Triuranium octaoxide ($U_3O_8$, National Bureau of Standards, 99.9%) was used in dissolution studies as a uranium-bearing standard reference material. Curcumin ($C_{21}H_{20}O_6$, TCI America, crystals), Triton-X-100 ($C_{14}H_{22}O(C_2H_4O)_{n(n=9-10)}$, VWR International, Reagent grade), sodium acetate ($NaOOCCH_3$, Alfa Aesar, 99%), acetic acid ($CH_3COOH$, VWR International, 99.7%), and uranyl acetate($UO_2(CH_3COO)_2•2H_2O$, Baker Analyzed, 99.4%) were used in the experiments of detecting uranyl cation according to the methods reported in Zhu et al.[3]

**Table S1: Composition of the Simulated Lung Fluids[2]**

| Composition ($g·L^{-1}$) | GS | ALF |
|---|---|---|
| **NaCl** | 6.779 | 3.21 |
| **$Na_2HPO_4$** | | 0.071 |
| **$NaHCO_3$** | 2.268 | |
| **Trisodium citrate dihydrate** | 0.055 | 0.077 |
| **$NH_4Cl$** | 0.535 | |
| **Glycine** | 0.375 | 0.059 |
| **$NaH_2PO_4$** | 1.872 | |
| **L-cysteine** | 0.121 | |
| **NaOH** | | 6.0 |
| **Citric acid** | | 20.8 |
| **$CaCl_2·2H_2O$** | 0.026 | 0.128 |
| **$Na_2SO_4$** | | 0.039 |
| **$MgCl_2·6H_2O$** | | 0.05 |
| **Disodium tartrate** | | 0.09 |
| **Sodium lactate** | | 0.085 |
| **Sodium pyruvate** | | 0.172 |
| **Properties** | | |
| **pH** | 7.3 ± 0.1 | 4.5 ± 0.1 |
| **Ionic strength ($mol·L^{-1}$)** | 0.17 | 0.34 |

Human respiratory tract can be divided into three major regions. These are extrathoracic or upper respiratory tract, tracheobronchial region and pulmonary or alveolar region, both together named as the lower respiratory tract. Particles that are smaller than 100μm can be entered the respiratory tract via inhalation. However, only the particles that are smaller than 10μm have the possibility of passing to the lower respiratory tract. The bigger particles may adsorb by the mucus and will be removed eventually. Some of these particles have the possibility of swallowing and entering the gastrointestinal tract. However, the smaller particles will be able to pass through these barriers and will move down the lower respiratory tract. The finest fraction, particles smaller than 4μm and nano particle aggregates has the possibility of penetrating into the alveolar region of the deep lungs. The alveolar region is the lung compartment where the oxygen – carbon dioxide gas exchange occurs. Hence, this area is in close contact with the blood vessels. Alveolar region contains three major types of cells. Type I cells that made up the structure, the Type II cells that secrete pulmonary surfactants to the alveolus and, alveolar macrophages which contain lysosomes and ready to consume foreign bodies that reach this region. The Gamble's solution (GS) is simulating the pulmonary surfactants secreting from Type II cells. The Artificial Lysosomal Fluid (ALF) solution simulates the conditions inside these alveolar macrophages when they engulf the foreign body, a process known as phagocytosis. The combined body is known as phagolysosome which contains the highly acidic environment required to destroy the foreign bodies.[4,5]

## Characterization of the Samples

### *BET Surface Area Analysis of the Samples*

Surface areas of samples were measured in a seven-point $N_2$-Brunauer-Emmet-Teller (BET) isotherm using a Quantachrome Autosorb-1 surface area analyzer. Samples were outgassed overnight (~24 h) at a temperature of 105°C prior to the BET analysis.

### *EPA-3052b Digestion Method[6]*

To determine the elemental concentrations of each dust sample an acid digestion procedure was followed. A 0.2 ±0.01 g subsample was weighed from each sample and placed in an individual digestion tube. Samples were sieved through 500μm sieve to remove organic debris prior to analysis. Three mL of trace-metal-grade hydrofluoric acid and 9mL of trace-metal-grade nitric acid were added to each digestion tube, and each tube was capped and placed in a holder. A preset microwave routine (Milestone EthosUP) included a 25 minute ramp to 180°C, after which the oven held that temperature for 10 minutes, consistent with the EPA 3052b digestion method.

### *Pre-concentration and XRD Analysis of the Uranium Minerals of the Dust Samples*

As the total %U of these samples are lower than 1% (the usual detection limit of the XRD analysis), a pre-concentration procedure was carried out. The dust samples were first sieved through a 500μm US standard sieve to remove debris. The uranium minerals in the samples are coatings around the quartz grains. Therefore, while sieving, the dust was lightly scratched using a porcelain pestle to scratch out the uranium minerals. Additional sieving was carried out using 120μm, 45μm and 20μm US standard sieves. The finest fraction collected was analyzed by XRD. Then, the spectra were compared with 15 different common uranium minerals in New Mexico along with common major minerals (i.e. quartz, kaolinite, microcline, dolomite, calcite, rutile). The presence of uranium minerals was confirmed only when their intensities and d – spacing were matched with respective standard patterns with at least five major peaks.

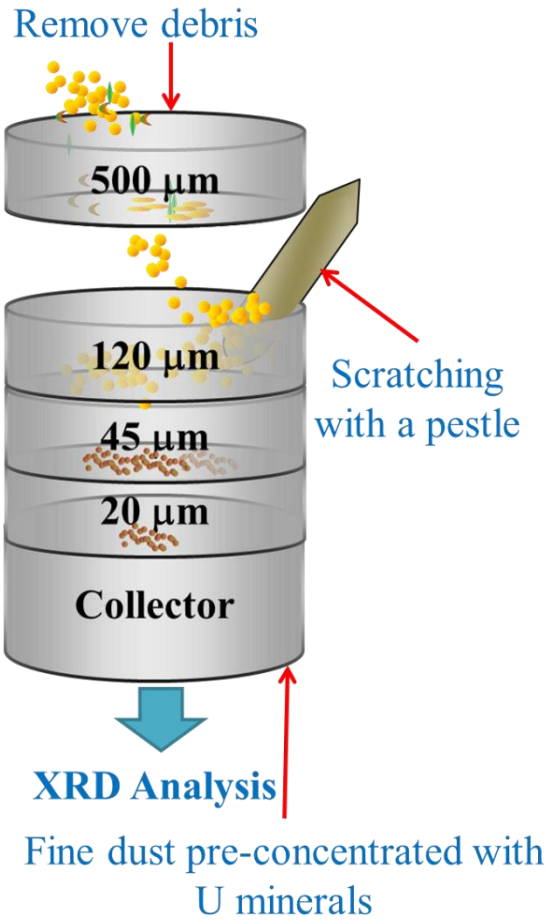


**Figure S2: Systematic diagram illustrating the pre-concentration procedure of uranium minerals**

***Particle Size Analysis***

Scanning Electron Microscope (SEM) images of the dust samples were analyzed using the software package ImageJ to obtain the particle sizes. The dust samples were first sonicated in isopropyl alcohol for 30 minutes to prevent aggregation and to obtain a well dispersed suspension. After air drying, the samples were sputter coated with Platinum and imaged with a NOVA-Nano-SEM-450. The obtained images were used to calculate the particle sizes.

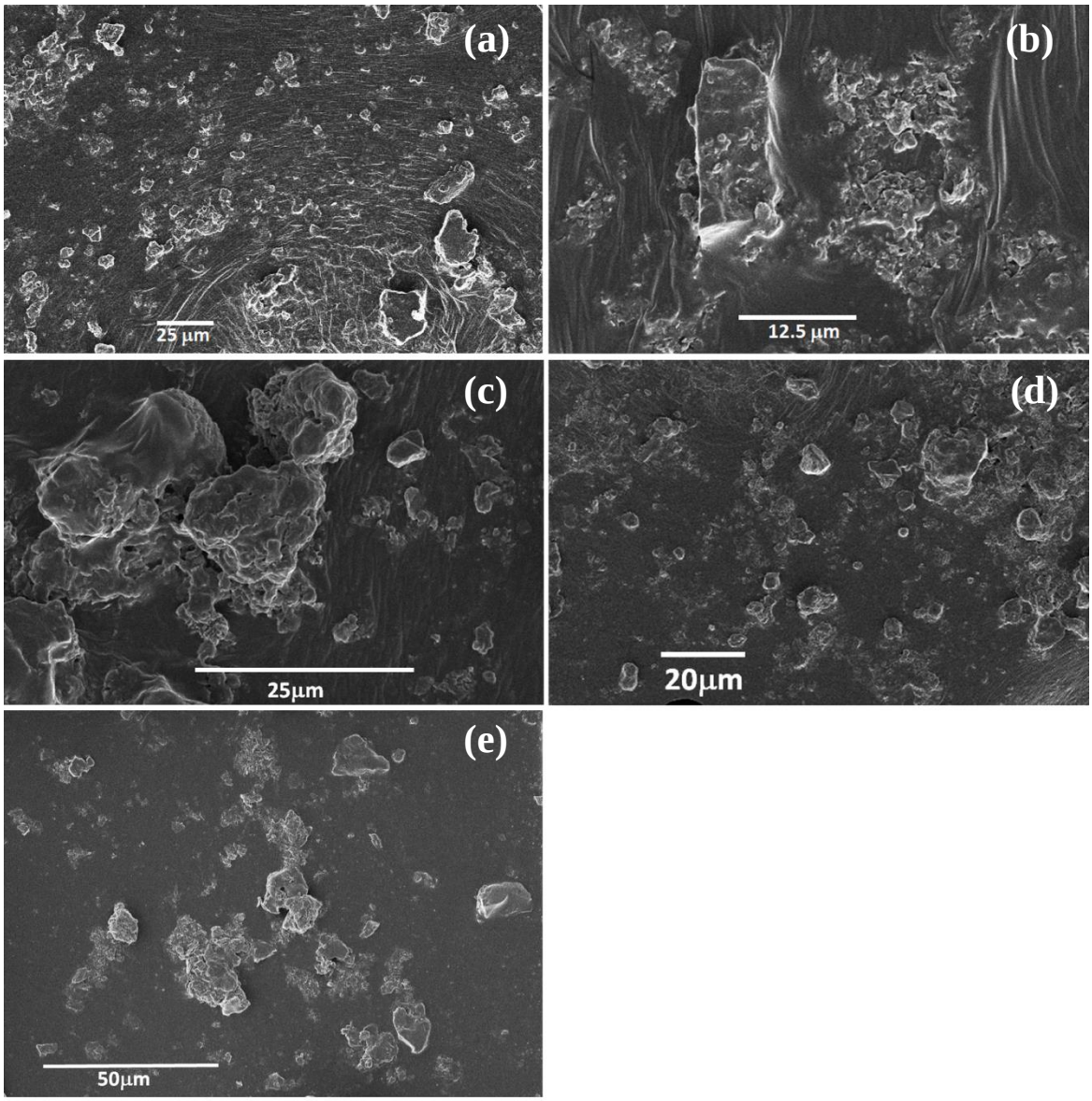


**Figure S3: SEM images of the samples of (a) Site A, (b) Site C, (c) Site E, (d) Site G, (e) St. Anthony**

**Table S2: Particle Sizes of the Samples and their Respective Number of $PM_{10}$, and $PM_4$ Particles as a Percentage of Total Number of Particles Analyzed**

| Sample | # of particles analyzed | Average length (µm) | $PM_{10}$ | $PM_4$ |
|---|---|---|---|---|
| **St. Anthony** | 424 | 4.6±4.0 | 90% | 57% |
| **A** | 520 | 4.7±4.6 | 88% | 61% |
| **C** | 421 | 3.4±4.6 | 92% | 75% |
| **E** | 418 | 4.0±4.8 | 89% | 74% |
| **G** | 380 | 3.9±3.3 | 94% | 69% |

Given below, **Figure S4** represents the particle size distribution as a function of size.

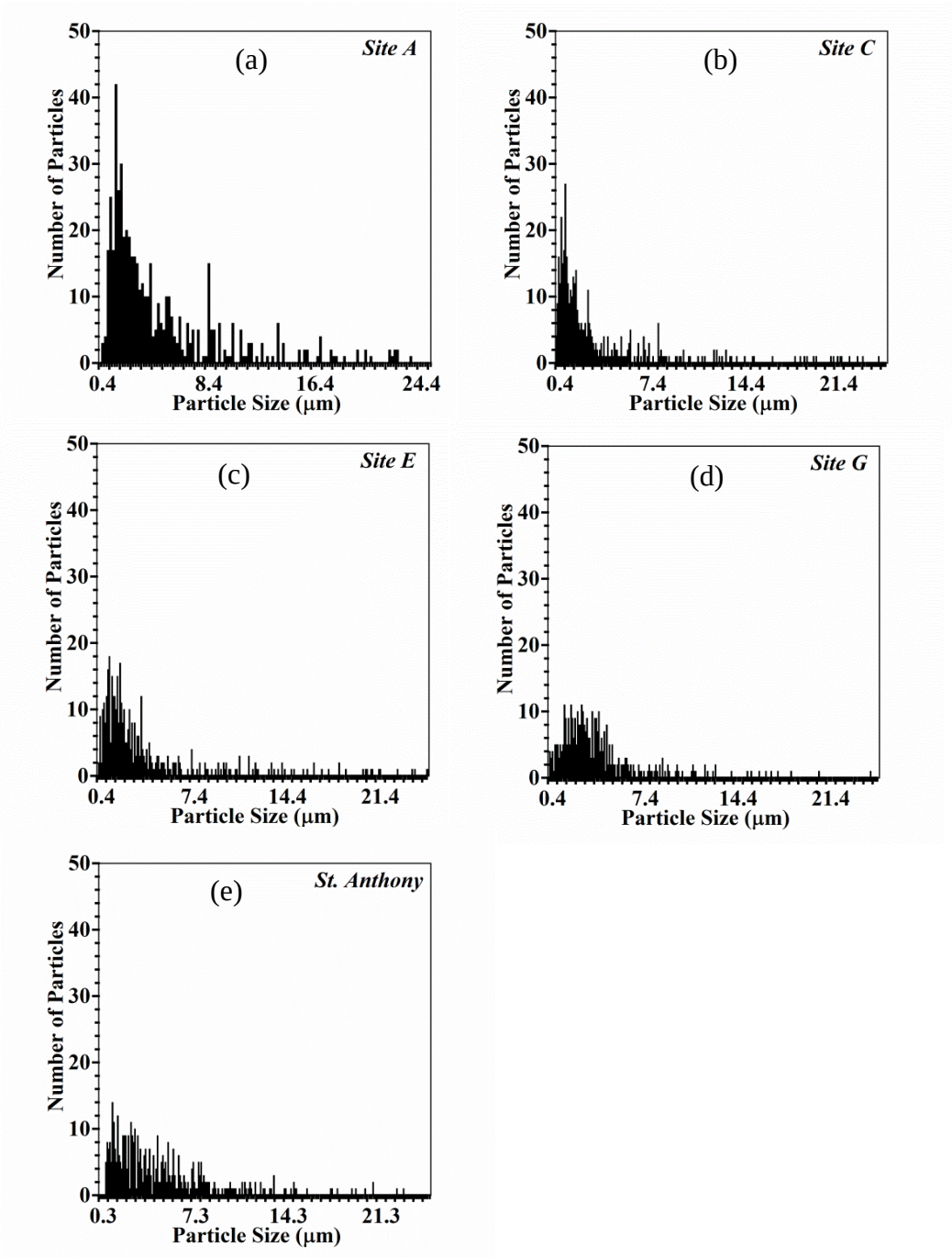


**Figure S4: Particle size distribution of the samples from (a) Site A, (b) Site C, (c) Site E, (d) Site G, and (e) St. Anthony. Larger standard deviation of the average length indicates a larger particle size distribution**.

**Table S3: Specific Surface Area Measurements and Total U% of the Analyzed Samples**

| Sample | Source of the samples | 7 points $N_2$ BET surface area ($m^2/g$) | %U |
|---|---|---|---|
| $U_3O_8$ | National Bureau of Standards, Assay: 99.9% | 0.46±0.04 | 85 |
| St. Anthony Sediment | St. Anthony Mine | 1.61±0.08 | 0.87 |
| Site A | Jackpile Mine | 2.10±0.09 | 0.23 |
| Site E | Jackpile Mine | 14.5±1.0 | 0.18 |
| Site C | Jackpile Mine | 0.77±0.14 | 0.14 |
| Site G | Jackpile Mine | 1.77±0.59 | 0.23 |

**Langmuir Type Model**

The Langmuir model fitting was done using inbuilt Langmuir Function (LangmuirEXT1) of OriginPro 8.

$$y = \frac{abx^{1-c}}{1 + bx^{1-c}}$$

where, **y** is the amount of total dissolved uranium, **x** is the reaction time, **a** is the maximum amount of total dissolved uranium, **b** is an equilibrium constant associated with the surface dissolution, and **c** is a co-efficient used to obtained the best fit (usually kept at 0).

**Table S4: Averaged Rates of U Dissolution for the First 3 hours and Percentage of U Dissolved in each SLF after 24 hour Exposure**

| Sample | Averaged rates of U dissolution for 1st 3 hours (μg $L^{-1}m^{-2}h^{-1}$) | | %U dissolved in SLF upon 24 hour exposure | |
|---|---|---|---|---|
| | GS | ALF | GS | ALF |
| **$U_3O_8$** | $3.9E^4$±1120 | $1.05E^6$±12101 | 0.743 | 16.162 |
| **St Anthony** | 104±3 | 233±6 | 0.700 | 1.801 |
| **Site A** | 5.0±0.1 | 4.6±0.2 | 0.036 | 0.043 |
| **Site C** | 1274±21 | 2017±36 | 11.086 | 7.873 |
| **Site E** | 3.2±0.2 | 2.0±0.2 | 0.297 | 0.173 |
| **Site G** | 63±1 | 184±5 | 0.810 | 1.367 |

**PHREEQC 3.3.8 Input (MINTEQ Database) of the Two Simulated Lung Fluids**

- The inbuilt MINTEQ database has used as the basic database. The other solid and aqueous species were imported from the other inbuilt databases (LLNL.dat, MINTEQ.v4.dat) within the model.

*GS Solution*

```
PHASES
Uranophane
    Ca(UO2)2(SiO3OH)2 + 6H+ = 2UO2+2 + Ca+2 + 2H4SiO4
    log_k     17.49
    delta_h   0 kcal
    -Vm       68.32 cm3/mol
SURFACE_MASTER_SPECIES
    Uranophane    Ca(UO2)2(SiO3OH)2
SURFACE_SPECIES
Ca(UO2)2(SiO3OH)2 = Ca(UO2)2(SiO3OH)2
    log_k     0
    delta_h   0 kJ
PHASES
Coffinite
    USiO4 + 4H+ = U+4 + H4SiO4
    log_k     -7.62
    delta_h   -14.548 kcal
    -Vm       68.32 cm3/mol
SURFACE_MASTER_SPECIES
    Coffinite     USiO4
    Quartz        SiO2
SURFACE_SPECIES
USiO4 = USiO4
    log_k     0
PHASES
Uranyl_carbonate
    Na4UO2(CO3)3 +3.0000 H+  =  + 1.0000 UO2++ + 3.0000 HCO3- + 4.0000 Na+
    log_k     4.0395
    delta_h   0 kcal
    -Vm       68.32 cm3/mol
SURFACE_MASTER_SPECIES
    Uranyl_carbonate Na4UO2(CO3)3
SURFACE_SPECIES
Na4UO2(CO3)3 = Na4UO2(CO3)3
    log_k     0
PHASES
Microcline
    KAlSi3O8 + 4H2O + 4H+ = 3H4SiO4 + Al+3 + K+
    log_k     0.616
    delta_h   -12.309 kcal
SURFACE_MASTER_SPECIES
    Microcline    KAlSi3O8
SURFACE_SPECIES
KAlSi3O8 = KAlSi3O8
    log_k     0
SURFACE_SPECIES
```

```
SiO2 = SiO2
    log_k     -3.9993
    delta_h   32.949 kJ
SOLUTION_MASTER_SPECIES
    Lactate       Lactate-         0     90.08           90.08

SOLUTION_SPECIES
Lactate- = Lactate-
    log_k     0
Lactate- + H+ = LactateH
    log_k     3.86
    delta_h   -1361.9 kJ

SOLUTION_MASTER_SPECIES
    Pyruvate      Pyruvate-        0     88.06           88.06
SOLUTION_SPECIES
Pyruvate- = Pyruvate-
    log_k     0
Pyruvate- + H+ = PyruvateH
    log_k     2.5
GAS_PHASE 1
    -fixed_pressure
    -pressure 1
    -volume 1
    -temperature 37
    O2(g)     1
EQUILIBRIUM_PHASES 1
    Quartz    0 0
    Microcline 0 0
    Dolomite(disordered) 0 0
    Kaolinite 0 0
    Rutile    0 0
    Calcite   0 0
    Uraninite 0 0
    Coffinite 0 0
    Autunite  0 0
    Uranyl_carbonate 0 0
    Torbernite 0 0
    Tyuyamunite 0 0
    Carnotite 0 0
    Uranophane 0 0
    Schoepite 0 0
SOLUTION 2
    temp      37
    pH        7.3
    pe        4
    redox     pe
    units     mmol/l
    density   1
    Na        159.2424
    Cl        126.4344
    Alkalinity 27
```

```
    Citrate   0.187
    N(-3)     10.0019
    Glycine   4.9953
    P         15.6026
    S(-2)     0.9987
    Ca        0.1769
    -water    0.1 # k
```

*ALF Solution*

```
PHASES
Uranophane
    Ca(UO2)2(SiO3OH)2 + 6H+ = 2UO2+2 + Ca+2 + 2H4SiO4
    log_k     17.49
    delta_h   0 kcal
    -Vm       68.32 cm3/mol
SURFACE_MASTER_SPECIES
    Uranophane    Ca(UO2)2(SiO3OH)2
SURFACE_SPECIES
Ca(UO2)2(SiO3OH)2 = Ca(UO2)2(SiO3OH)2
    log_k     0
    delta_h   0 kJ
PHASES
Coffinite
    USiO4 + 4H+ = U+4 + H4SiO4
    log_k     -7.62
    delta_h   -14.548 kcal
    -Vm       68.32 cm3/mol
SURFACE_MASTER_SPECIES
    Coffinite     USiO4
    Quartz        SiO2
SURFACE_SPECIES
USiO4 = USiO4
    log_k     0
PHASES
Uranyl_carbonate
    Na4UO2(CO3)3 +3.0000 H+  =  + 1.0000 UO2++ + 3.0000 HCO3- + 4.0000 Na+
    log_k     4.0395
    delta_h   0 kcal
    -Vm       68.32 cm3/mol
SURFACE_MASTER_SPECIES
    Uranyl_carbonate Na4UO2(CO3)3
SURFACE_SPECIES
Na4UO2(CO3)3 = Na4UO2(CO3)3
    log_k     0
PHASES
Microcline
    KAlSi3O8 + 4H2O + 4H+ = 3H4SiO4 + Al+3 + K+
    log_k     0.616
    delta_h   -12.309 kcal
SURFACE_MASTER_SPECIES
    Microcline    KAlSi3O8
SURFACE_SPECIES
```

```
KAlSi3O8 = KAlSi3O8
    log_k     0
SURFACE_SPECIES
SiO2 = SiO2
    log_k     -3.9993
    delta_h   32.949 kJ
SOLUTION_MASTER_SPECIES
    Lactate       Lactate-         0     90.08           90.08

SOLUTION_SPECIES
Lactate- = Lactate-
    log_k     0
Lactate- + H+ = LactateH
    log_k     3.86
    delta_h   -1361.9 kJ

SOLUTION_MASTER_SPECIES
    Pyruvate      Pyruvate-        0     88.06           88.06
SOLUTION_SPECIES
Pyruvate- = Pyruvate-
    log_k     0
Pyruvate- + H+ = PyruvateH
    log_k     2.5
GAS_PHASE 1
    -fixed_pressure
    -pressure 1
    -volume 1
    -temperature 37
    O2(g)     1
EQUILIBRIUM_PHASES 1
    Quartz    0 0
    Microcline 0 0
    Dolomite(disordered) 0 0
    Kaolinite 0 0
    Rutile    0 0
    Calcite   0 0
    Uraninite 0 0
    Coffinite 0 0
    Autunite  0 0
    Uranyl_carbonate 0 0
    Torbernite 0 0
    Tyuyamunite 0 0
    Carnotite 0 0
    Uranophane 0 0
    Schoepite 0 0
SOLUTION 2
    temp      37
    pH        4.5
    pe        4
    redox     pe
    units     mmol/l
    density   1
```

```
Ca         0.8707
Citrate    99.2444
Cl         57.1991
Glycine    0.7859
Lactate    0.7585
Mg         0.2459
Na         211.0301
P          0.807
Pyruvate   1.5636
S(6)       0.2746
Tartarate  0.3912
-water     0.1 # kg
```

**Table S5: The Initial Mineral Molar Ratios of the each Site used in PHREEQC3.3.8; Intensities were Based on the Observed Intensities in XRD Analysis**

| Bulk mineralogy | Uranium mineralogy | St. Anthony Sediment | Site A | Site C | Site E | Site G |
|---|---|---|---|---|---|---|
| **Quartz** | | 99 | 99 | 99 | 99 | 99 |
| **Dolomite** | | 1 | 1 | 1 | 1 | 1 |
| **Kaolinite** | | 1 | 1 | 0 | 0 | 1 |
| **Microcline** | | 0 | 1 | 0.01165 | 0.012 | 1 |
| **Calcite** | | 0 | 0 | 1 | 1 | 1 |
| **Rutile** | | 1 | 0 | 0 | 0 | 0 |
| | **Uraninite** | 0.01 | 0 | 0.06 | 0.02 | 0.002 |
| | **Coffinite** | 0.01 | 0 | 0.0065 | 0.005 | 0.0025 |
| | **Andersonite** | 0 | 0 | 0.015 | 0.00012 | 0.0005 |
| | **Autunite** | 0.08 | 0.01 | 0.012 | 0.01 | 0.005 |
| | **Torbentite** | 0 | 0.01 | 0 | 0.005 | 0.0005 |
| | **Tyuyamunite** | 0 | 0 | 0 | 0 | 0.00001 |
| | **Carnotite** | 0 | 0 | 0.005 | 0.001 | 0 |
| | **Uranophane** | 0.001 | 0 | 0 | 0 | 0 |
| | **Schoephite** | 0.1 | 0 | 0 | 0 | 0 |

**Table S6: Modeled Equilibrium Concentrations of Dissolved Uranium for Different Uranium Minerals in each SLF using PHREEQC3.3.8. The dissolution was Modeled by Introducing only One Uranium Containing Mineral at a Time.**

| Mineral | Dissolved U concentration (M) | | |
|---|---|---|---|
| | ALF | GS | GS/ALF |
| **Autunite** | 1.028E-02 | 1.626E-02 | 1.58 |
| **Carnotite** | 4.044E-04 | 6.513E-03 | 16.11 |
| **Schoephite** | 2.170E-02 | 1.252E-02 | 0.58 |
| **Torbernite** | 6.078E-02 | 1.574E-02 | 0.26 |
| **Tyuyamunite** | 4.052E-04 | 7.207E-03 | 17.79 |
| **Uraninite** | 7.074E-01 | 7.081E-01 | 1.01 |
| **Coffinite** | 8.166E-01 | 7.792E-01 | 0.95 |
| **Uranophane** | 4.627E-02 | 1.186E-02 | 0.26 |

**Table S7: Modeled Equilibrium Concentrations of Dissolved Uranium for each Site in each SLF Using PHREEQC3.3.8**

| Site | Dissolved U concentration (M) | | |
|---|---|---|---|
| | ALF | GS | GS/ALF |
| **Site A** | 1.654E-01 | 3.498E-02 | 0.211 |
| **Site C** | 9.307E-01 | 1.128E+00 | 1.212 |
| **Site E** | 2.499E-01 | 2.919E-01 | 1.168 |
| **Site G** | 7.551E-02 | 3.426E-02 | 0.454 |
| **St. Anthony** | 5.940E-02 | 1.174E-02 | 0.198 |

**Table S8: Percentage of each Uranium Mineral Dissolved in the Two SLFs and the Percentage Contribution of each Mineral to the Extent of Total Dissolved Uranium Concentration at Equilibrium. The Percentage of each Mineral Dissolved in each Site was obtained from the PHREEQC3.3.8. The Percentage Contributions from each Mineral at Equilibrium were obtained using Mass Balance Equations, Constructed using Modeled Data with Experimentally obtained Extents of Dissolutions.**

| Site | Major uranium minerals identified | % of the mineral dissolved (amount in the solution phase at equilibrium) | | % Contribution to the total dissolved U concentration at equilibrium | |
|---|---|---|---|---|---|
| | | ALF | GS | ALF | GS |
| St. Anthony | Uraninite | 100 | 100 | 8 | 10 |
| | Coffinite | 100 | 100 | 8 | 10 |
| | Autunite | 0.02 | -1* | 0.02 | 0 |
| | Uranophane | 10 | 10 | 0.2 | 0.2 |
| | Schoepite | 14 | 10 | 81.98 | 79.8 |
| Site A | Autunite | -14* | 4 | 0 | 30 |
| | Torbernite | 100 | 12 | 100 | 70 |
| Site C | Uraninite | 100 | 100 | 66 | 51 |
| | Coffinite | 100 | 100 | 7 | 6 |
| | Andersonite | 100 | 100 | 16 | 13 |
| | Autunite | -61* | 100 | 0 | 21 |
| | Carnotite | 100 | 100 | 11 | 9 |
| Site E | Uraninite | 100 | 100 | 56.96 | 53.34 |
| | Coffinite | 100 | 100 | 14.24 | 13.33 |
| | Andersonite | 92 | 0 | 0.31 | 0 |
| | Autunite | -50* | 10 | 0 | 5.33 |
| | Torbernite | 100 | 100 | 28.48 | 26.67 |
| | Carnotite | 0.02 | 25 | 0.001 | 1.32 |
| Site G | Uraninte | 100 | 100 | 26 | 33 |
| | Coffinite | 100 | 100 | 33 | 42 |
| | Andersonite | 100 | 100 | 7 | 8 |
| | Autunite | 16 | -10* | 21 | 0 |
| | Torbernite | 100 | 100 | 13 | 17 |
| | Tyuyamunite | 0.005 | 0.00012 | 0.00001 | 0.01 |

* A negative number of the amount of moles dissolved indicates the particular mineral precipitates under the conditions considered.

**The pH of the Solutions throughout the Dissolution Experiments**

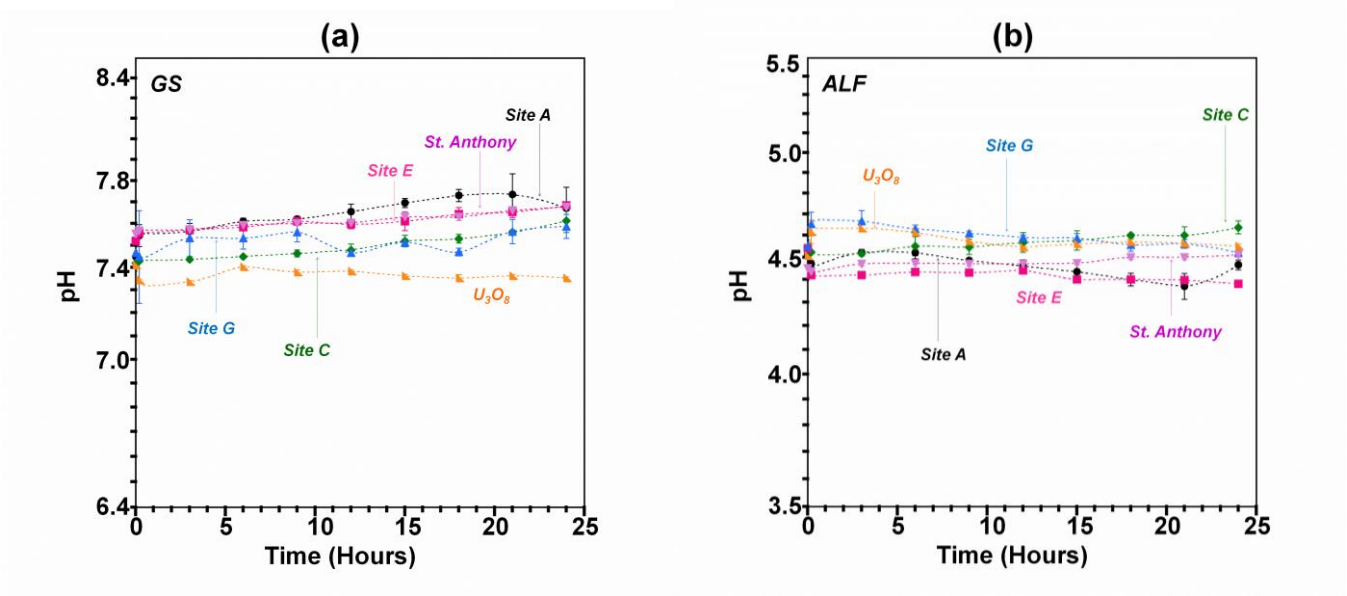


**Figure S5: The variation of pH of the solutions (a) GS (b) ALF through the dissolution experiment**

**Detection of the $UO_2^{2+}$ in Reacted Simulated Lung Fluids**

Uranyl-Curcumin-Triton-X System was prepared according to the method described by Zhu et al.[3] The calibration standards were prepared using 400 μM stock uranyl acetate solution prepared in GS and ALF matrices instead of MilliQ water matrix. However, the UV-VIS absorption of two stock solutions made on SLFs was compared with a MilliQ water based stock solution using Evolution 200 UV – Visible Spectrometer to confirm that there is no significant interference from the matrix. The calibration plots are provided in the **Figure S6**.

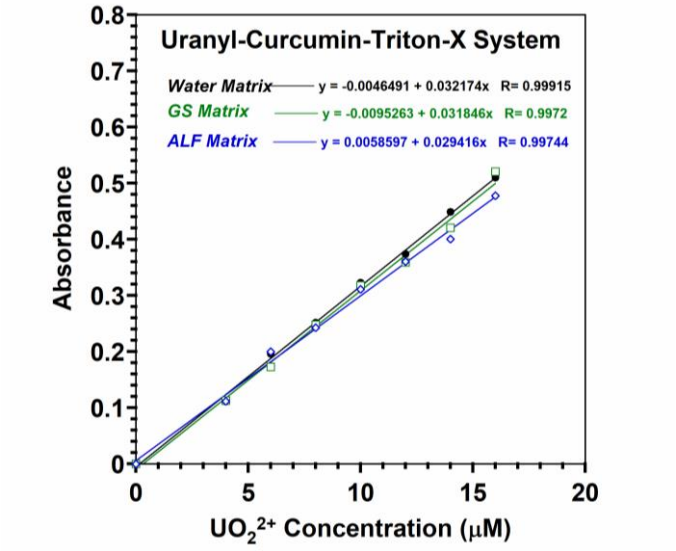


**Figure S6: The calibration curve for Uranyl-Curcumin-Triton-X system, UV/ VIS absorption at 430 nm, standard solutions were prepared in MilliQ water, GS and ALF.**

Colorimetric analysis qualitatively determined (orange coloration) all the samples contained $UO_2^{2+}$ in the solutions.

**Persistence through the Seasons**

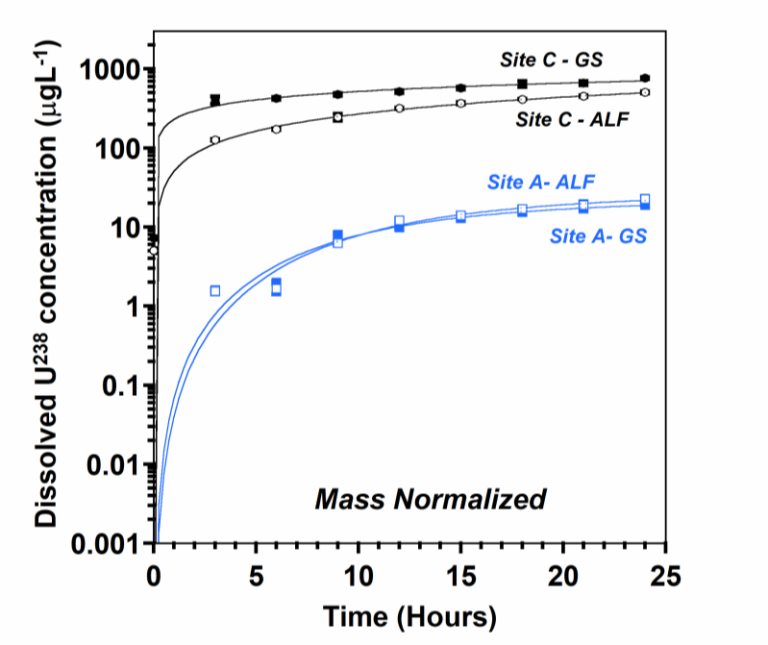


**Figure S7: The dissolution of total uranium (TDU) from the two Sites A and C collected during the winter 2017, in the two SLFs as a function of time. Data has been normalized to their respective surface areas (Site A = 2.1±0.3 $m^2g^{-1}$, Site C = 0.90±0.1 $m^2g^{-1}$) and are fitted to Langmuir type model and presented with log scaled Y Axis (Total Dissolved U Concentration µg $L^{-1}$)**

**References**


1. Brown, R. D. Geochemistry and Transport of Uranium-Bearing Dust at Jackpile Mine, Laguna, New Mexico, Master's Thesis, New Mexico Institute of Mining and Technology, Socorro, New Mexico, August 2017.
2. Pelfrêne, A.; Cave, M. R.; Wragg, J.; Douay, F. In vitro investigations of human bioaccessibility from reference materials using simulated lung fluids. *Int. J. Environ. Res. Public Health* **2017**, *14*, 1–15.
3. Zhu, J. H.; Zhao, X.; Yang, J.; Tan, Y. T.; Zhang, L.; Liu, S. P.; Liu, Z. F.; Hu, X. L. Selective colorimetric and fluorescent quenching determination of uranyl ion via its complexation with curcumin. *Spectrochim. Acta - Part A Mol. Biomol. Spectrosc.* **2016**, *159*, 146–150.
4. Kastury, F.; Smith, E.; Juhasz, A. L. A critical review of approaches and limitations of inhalation bioavailability and bioaccessibility of metal(loid)s from ambient particulate matter or dust. *Sci. Total Environ.* **2017**, *574*, 1054–1074.
5. Stine, K.; Brown, T. *Principles of Toxicology*, 1st ed.; CRC Lewis: New York, 2010.
6. Environmental Protection Agency, U. EPA Method 3050B (SW-846): Acid Digestion of Sediments, Sludges, and Soils. 1996.